Trace element fractionation during fluid-induced eclogitization in a subducting slab: trace element and Lu–Hf–Sm–Nd isotope systematics

Timm John[a,b,*], Erik E. Scherer[b], Karsten Haase[a], Volker Schenk[a]

[a]*Institut für Geowissenschaften and SFB 574, Universität Kiel, Olshausenstr. 40, 24098 Kiel, Germany*
[b]*Institut für Mineralogie, Universität Münster, Corrensstr. 24, 48149 Münster, Germany*

Abstract

Spatially closely associated gabbros and eclogites of central Zambia represent relics of subducted oceanic crust in a suture zone. The eclogites, which formed at 630–690 °C and 2.6–2.8 GPa, yield Lu–Hf ages between 607 ± 14 and 659 ± 14 Ma, suggesting that subduction was active for at least 24 Myr. The trace element- and isotope compositions of the gabbros and eclogites range from those of incompatible-element depleted gabbros from the lower oceanic crust to those of enriched ocean–island basalts. Several eclogites display a large fractionation of the light rare earth elements from heavy rare earth- and high field strength elements, an effect that cannot be of magmatic origin but must have resulted from the passage of fluids through the rocks during metamorphism. In some samples, fluid pathways are marked by veins of eclogite facies minerals. Garnet-whole rock ages based on the Sm–Nd (relatively mobile) and Lu–Hf (relatively immobile) systems are identical, consistent with light rare earth elements being fractionated during eclogitization. Modeling using fluid–mineral partition coefficients suggests that the fractionated rocks have reacted with an amount of fluid equal up to 80% of their mass. The most likely source for such a large volume of fluid is the serpentinized lithospheric mantle of the subducting slab. The Zambian eclogites and their veins represent relict fluid pathways through subducted oceanic crust and provide direct evidence for channelized fluid flow and element transport within a slab. The transformation of dry, metastable slab gabbros to eclogites upon fluid-infiltration, accompanied by the transport of fluid-mobile elements, could be responsible for generating the slab component in arc magmas.
© 2004 Elsevier B.V. All rights reserved.

  * Corresponding author. Institut für Geowissenschaften and SFB 574, Universität Kiel, Olshausenstr. 40, 24098 Kiel, Germany. Tel.: +49 0 431 8802864; fax: +49 431 880 4457.
  E-mail addresses: tj@min.uni-kiel.de (T. John), escherer@nwz.uni-muenster.de (E.E. Scherer), kh@gpi.uni-kiel.de (K. Haase), vs@min.uni-kiel.de (V. Schenk).

1. Introduction

The dehydration of subducting oceanic lithosphere is one of the main processes currently producing element fractionation within the Earth. Fluids released by dehydration trigger metamorphism within subduction zones (e.g., eclogite formation [1–3]), and magma generation in the overlying mantle wedge (e.g., [4,5]). Many workers have postulated fluid flow out of subducting slabs to explain the characteristic enrichment of fluid-mobile elements relative to fluid-immobile elements in magmatic rocks from convergent margins [6,7]. To better understand the origin of this arc signature, knowledge about (1) the fluid–rock interactions within the subducting slab and (2) the fluid flux into the mantle wedge is required. The rocks of subducting slabs transform to high-pressure (HP)/low-temperature (LT) metamorphic rocks (e.g., basaltic rocks transform to eclogites). Thus, the occurrence of eclogites having compositions similar to those of mid-ocean ridge basalts (MORB) indicates specific plate-tectonic processes that lead to the completion of a Wilson cycle [8]. However, trace element signatures, which are used to identify specific geologic settings in which the eclogite precursors formed, are often obscured by metamorphism, including the gabbro-to-eclogite transformation process itself. Low-temperature metamorphism is mainly controlled by the presence of fluids, which catalyze the mineral–chemical reactions and transports elements (e.g., [2]). Consequently, only relatively fluid-immobile trace elements, such as the rare earth elements (REE) and high field strength elements (HFSE), can be applied to reconstruct compositions of the basaltic and gabbroic precursors (e.g., [8–10]). However, several studies have shown that the light-REE (LREE) are mobilized during HP/LT metamorphism [11–13], casting doubt on their usefulness for determining protolith compositions. Moreover, fractionation of the LREE by fluids may disturb Sm–Nd ages if the fluid flow took place significantly later than metamorphism.

This study focuses on the geochemistry of Zambian eclogites and associated gabbros, which are interpreted to be relics of a fossil subducted slab [8]. Within these rocks, gradual stages of prograde gabbro-to-eclogite transformation are preserved by disequilibrium textures of incomplete reactions. The main processes that transformed the Zambian gabbros to eclogites are fluid-controlled dissolution, transport, and precipitation [3,14], demonstrating the importance of fluid–rock interaction in low-T environments. Because the Zambian eclogites and gabbros are cogenetic and belonged to the same subducted plate [3,8], they provide an exceptional opportunity to study the influence of fluid-induced metamorphic processes on the bulk geochemistry of subducting gabbroic rocks. Our goals are (1) to investigate the mobility of trace elements during eclogitization, and (2) to date the metamorphism and element transport in the Zambian eclogites using combined Lu–Hf and Sm–Nd isotope systematics.

2. Geologic setting and sample characterization

The Zambian eclogites occur within the Zambezi Belt, which is part of a Pan-African orogenic system between the Congo and Kalahari Cratons (Fig. 1). These Pan-African belts are interpreted to have formed during the break-up of Rodinia and the assembly of Gondwana [15,16]. Subduction and thus eclogite facies metamorphism (630–690 °C and 2.6–2.8 GPa [3]) occurred during the convergence of the Kalahari and the Congo cratons until ca. 600 Ma [8], whereas the peak metamorphism during the subsequent continental collision reached the HP amphibolite facies at ca. 530 Ma (e.g., [15,17,18]). Detailed descriptions of the geologic setting, rock textures, and mineral chemistry of the Zambian eclogites are given elsewhere [3,8,19] and will be only briefly summarized here. The eclogites, together with metagabbros, gabbros, and rare ultramafic rocks, form isolated hills of 10 to 100 m in diameter within a 200-km long by up to 40-km wide zone along the central axis of the Zambezi Belt (Fig. 1). No contacts between the eclogites and the other mafic rocks or the country rocks are exposed. This area is interpreted to be part of a late Precambrian suture zone, with the mafic rocks being relics of the subducted gabbroic part of the lower oceanic crust. The mafic rocks and their present country rocks were juxtaposed during continental collision, 70 Myr after subduction of oceanic lithosphere ceased.

Along with fully equilibrated eclogites, the sample suite also includes partially eclogitized rocks that contain magmatic pyroxene relics and disequilibrium textures indicative of incomplete reactions. In such rocks, complete eclogitization occurred only in mm-
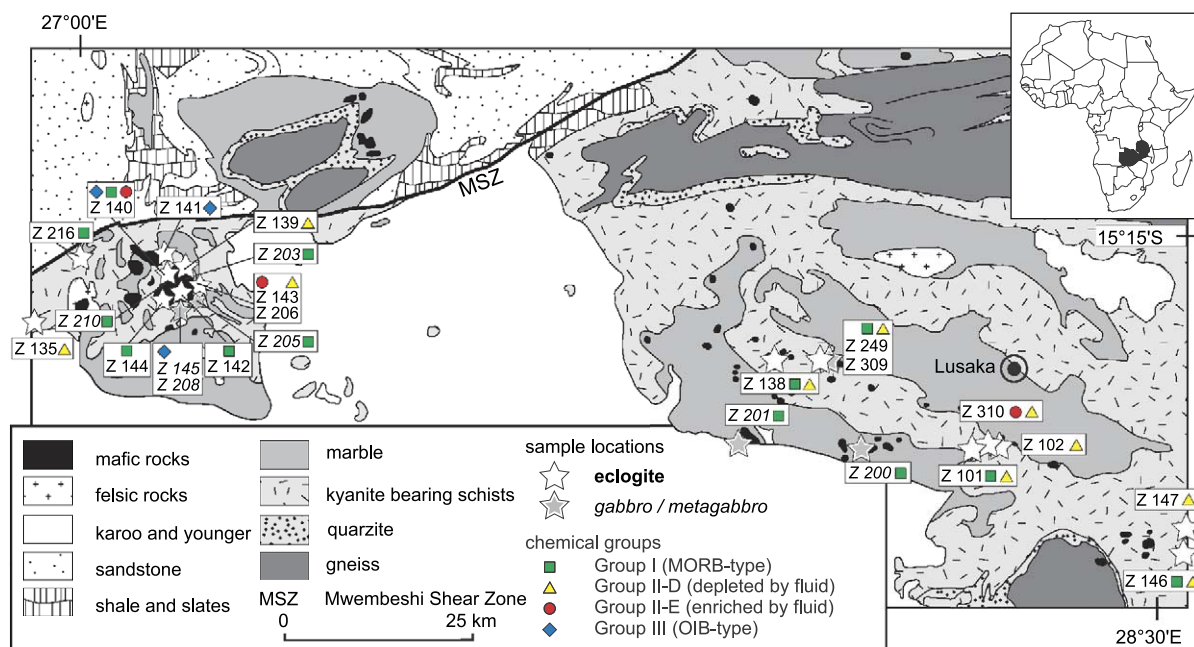
Fig. 1. Simplified geological map of central Zambia after Thieme [56] showing sample locations. Eclogite (±gabbro) occurrences are indicated by open stars and bold sample numbers; gabbro-only occurrences are indicated by filled stars and italic sample numbers. Symbols next to sample numbers indicate the chemical groups found at each locality.

to cm-sized volumes. We refer to all plagioclase-free samples that have at least some domains of the critical assemblage garnet+omphacite as eclogites. Though equilibrium was apparently reached within these small domains, disequilibrium on a larger scale is implied by the presence of kyanite in Al-poor (MORB-like) eclogites [3]. Eclogites that were not pervasively deformed typically preserve features of their original gabbroic texture, with eclogite facies minerals pseudomorphically replacing plagioclase and pyroxene. Textures of the deformed eclogites range from sheared porphyroclastic to porphyroblastic. No evidence for prograde blueschist- or amphibolite facies mineral assemblages was found. Instead, the pseudomorphic replacement of plagioclase by fine-grained intergrowths of omphacite, garnet, kyanite, and quartz strongly suggests that the gabbroic precursors were eclogitized directly without any significant intervening metamorphic reactions. Eclogitization was catalyzed by a channelized fluid flow that formed veins of eclogite facies minerals [3]. The spatial proximity of the Zambian eclogites and the gabbros, their similar trace element patterns and Nd isotope compositions, and the presence of relict magmatic minerals and gabbroic textures of the eclogites, all suggest that the gabbros and eclogites are cogenetic and followed similar pressure–temperature–time ($P–T–t$) paths, i.e., both were subducted to eclogite facies conditions and then rapidly exhumed before delicate HP intergrowth textures could re-equilibrate at lower $P–T$ conditions [3,8]. The degree of eclogitization in each sample depended on the availability of reaction-catalyzing fluids: Full eclogitization occurred only if sufficient fluid was available during the entire reaction interval, whereas partial eclogitization resulted if the fluid left the system before the reactions were complete. Gabbros remained unreacted under fluid-absent conditions.

3. Analytical methods

Thirty-four eclogite and 13 gabbro/metagabbro samples from 21 localities were chosen for major and trace element analyses (Supplementary Table 1). Eleven samples were also analyzed for their Sm–Nd and Lu–Hf isotopic compositions. Whole rocks were crushed with a steel jaw crusher and then powdered in

an agate mill. Garnet separates from three localities were prepared using a steel jaw crusher, disk mill, magnetic separator, and handpicking. To remove surface contamination, garnets were washed for 10 min in cold 1 M HCl, and rinsed with distilled water. Major elements were analyzed with a Philips 1400 XRF spectrometer at Kiel University (Supplementary Table 1). Trace elements were analyzed by first dissolving the samples using a lithium borate fusion procedure, then measuring after the method described by Garbe-Schönberg [20] using an upgraded Plasma-quad PQ1 ICP-MS (Kiel). Analyses of standards measured together with the samples indicate that the precision and accuracy of the trace element concentrations are better than 5%.

The Lu–Hf and Sm–Nd analyses were carried out at the Zentrallabor für Geochronologie in Münster. All samples were spiked with mixed ^{180}Hf–^{176}Lu and ^{149}Sm–^{150}Nd tracers before digestion with HF–HNO$_3$–HClO$_4$ in steel-jacketed Teflon bombs at 180 °C. Chemical separation procedures for Lu–Hf and Sm–Nd follow those of [21–23]. Lutetium and Hf were analyzed in static mode on the Micromass Isoprobe (Münster), whereas most Sm and Nd analyses were measured on the VG Sector 54 mass spectrometer (Münster) using static and dynamic modes, respectively. Hafnium and Nd isotope ratios were corrected for mass bias using ^{179}Hf/^{177}Hf=0.7325, and ^{146}Nd/^{144}Nd=0.7219, and the exponential law. Admixed Re was used to apply an external mass bias correction to the Lu isotope dilution measurements. Measured ^{176}Hf/^{177}Hf and ^{143}Nd/^{144}Nd values are reported relative to ^{176}Hf/^{177}Hf=0.282163 for the Münster Ames Hf standard (isotopically indistinguishable from JMC-475), and ^{143}Nd/^{144}Nd=0.511858 for the La Jolla Nd standard. Procedural blanks for Lu, Hf, Sm, and Nd were <20, <30, <50, and <200 pg, respectively. Calculated ages and initial isotope compositions are based on the decay constants λ^{176}Lu= 1.865×10^{-11} year^{-1} [24], and λ^{147}Sm=6.54×10^{-12} year^{-1} [25] and references therein. The chondritic uniform reservoir (CHUR) parameters used for calculating initial ε_{Hf} and ε_{Nd} values are ^{176}Hf/^{177}Hf= 0.282772 [26], ^{176}Lu/^{177}Hf=0.0332 [26], ^{143}Nd/ ^{144}Nd=0.512638 ([27] recalculated with updated oxygen isotope data [28] and using ^{146}Nd/^{144}Nd=0.7219 to correct for mass fractionation), and ^{147}Sm/^{144}Nd= 0.1967 [27].

4. Results

4.1. Major and trace elements

All samples have basaltic compositions with 45–52 wt.% SiO$_2$ and together, they display tholeiitic differentiation trends, with Fe- and Ti-enrichment in the early stages of fractionation. Distinguishing among the possible upper mantle settings in which the tholeiitic basalts may have been generated, e.g., ocean floor spreading axes, island arcs, or mantle plumes, requires further characterization using trace elements. On the basis of their chondrite-normalized REE and MORB-normalized trace element patterns, the mafic rocks of central Zambia were divided into three groups: The first has LREE-depleted patterns, the second has unusual REE patterns with large variations in LREE concentrations, and the third is LREE-enriched (Fig. 2).

Group I includes 19 samples from 12 localities spread across the whole study area (Fig. 1; Supplementary Table 1). Their (La/Sm)$_N$ ratios of <1 are similar to those of average normal MORB (N-MORB), and their heavy REE (HREE) concentrations are 7 to 30 times chondritic values (Fig. 2a). The trace element patterns of some Group I samples are comparable to those of recent MORBs (Fig. 2b), whereas other samples are as highly depleted as the basalts from the Garrett Fracture Zone in the SE Pacific [29]. Some samples have a slightly negative Eu anomaly (Fig. 2a).

Group II consists only of eclogites (n=21) from 11 localities (Supplementary Table 1, Fig. 1), whereas the other groups contain both gabbro and eclogite samples. The characteristic feature of Group II is an unusual decoupling of LREE (La to Gd) from the HREE and HFSE. Most samples in this group are LREE-depleted (=Group II-D, Fig. 2c), yielding 's'-shaped REE patterns, while four samples from localities Z143, 140, and 310 display LREE enrichments up to 30 times chondritic (=Group II-E, Fig. 3). Importantly, the MORB-normalized trace element patterns (Fig. 2d) indicate that only the LREE vary, whereas the HREE, together with the HFSE, Th, and P, which bracket the LREE in terms of relative mantle compatibility, occur in N-MORB-like concentrations. For example, the most extreme samples show about a seven-fold depletion of La, Ce, and Nd relative to Nb and P, resulting in large negative LREE anomalies.
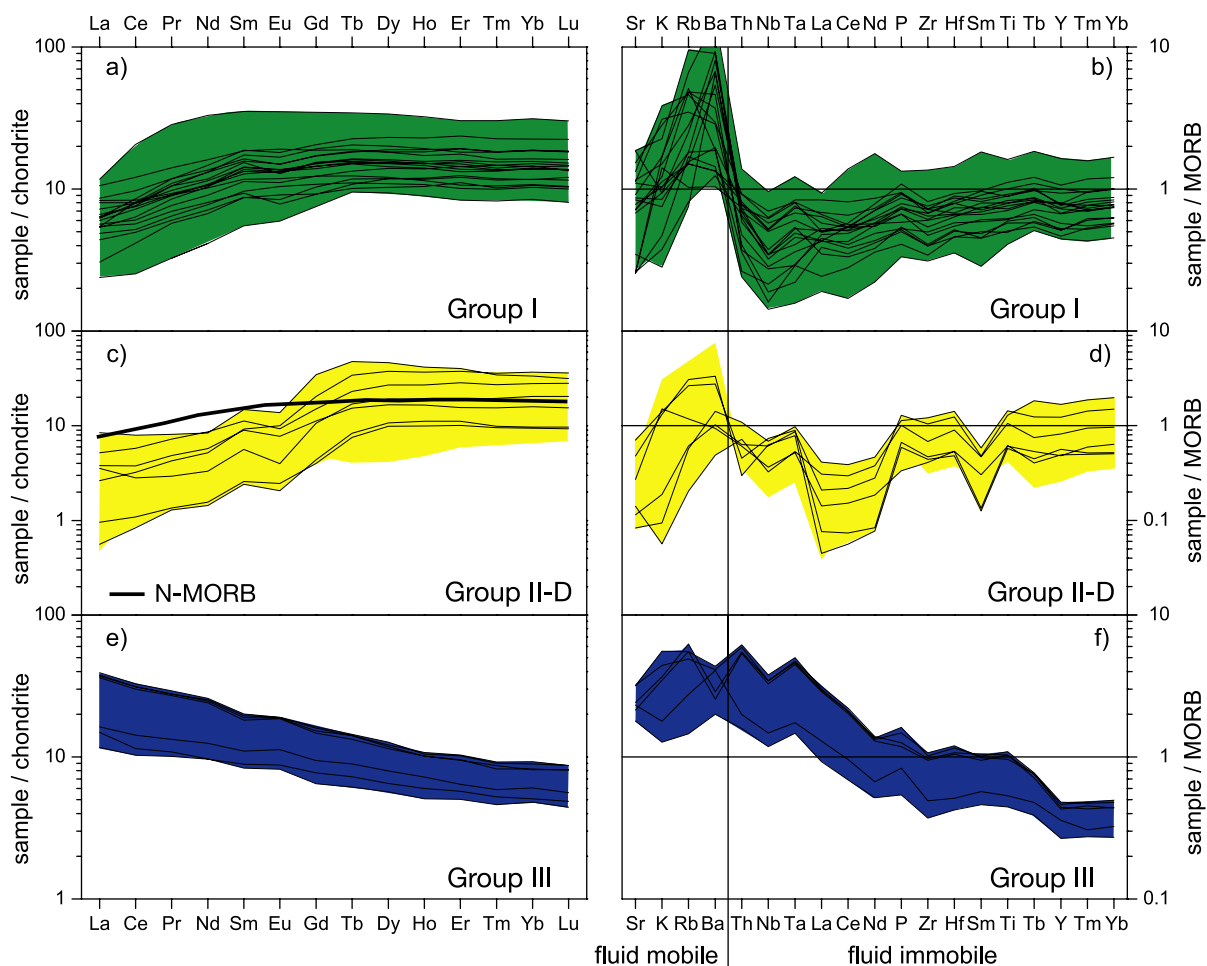
Fig. 2. (a, c, and e) Chondrite-normalized REE variation diagrams [57] for eclogites, gabbros, and metagabbros. (b, d, and f) Trace element variation plots, normalized to MORB [48] (*P* value from [58]). Some Group II patterns were omitted for clarity.

Group III comprises seven samples from three localities (Supplementary Table 1; Fig. 1). The chondrite-normalized REE patterns are smooth and have $(La/Sm)_N$ ratios >1, reflecting moderate LREE enrichment (10–40×chondrite) relative to that of the HREE (5–9×chondrite, Fig. 2e).

4.2. Lu–Hf and Sm–Nd isotope systematics and chronology

The Lu–Hf and Sm–Nd isotope compositions of five Group I gabbros and six eclogites from Groups I and II were analyzed (Supplementary Table 2). The LREE fractionation effects on Sm/Nd ratios in the

Zambian eclogites are evident when compared to modern basalt compositions on a plot of $^{176}Lu/^{177}Hf$ vs. $^{147}Sm/^{144}Nd$ (Fig. 4a), which has been used elsewhere to screen metabasites for altered samples [30]. Whereas Group I samples generally resemble the modern basalts, most Group II-D eclogites have higher Sm/Nd than basalts for any given Lu/Hf ratio. Group III samples lie within the field of ocean island basalts (OIB) or enriched MORB (Fig. 4a).

A 0.72 ± 0.10 Ga Sm–Nd isochron (*n*=7, M.S.W.D.=1.1) defined by most Groups I and II gabbros and eclogites was interpreted to date the crystallization of the igneous precursors of these rocks [8]. The whole rock Lu–Hf data are consistent with
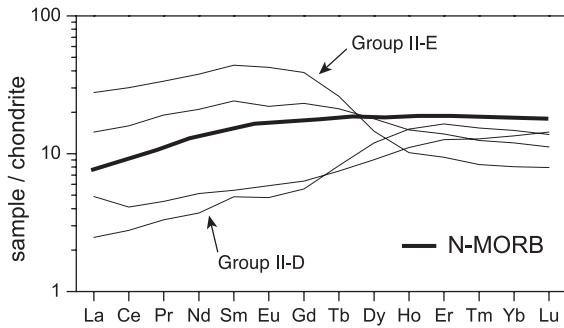
Fig. 3. Chondrite-normalized REE variation diagram [57] for eclogites from locality Z143 compared to N-MORB. Fluids have either depleted or enriched the samples in LREE relative to N-MORB. These depleted and enriched rocks represent sources and sinks, respectively, for fluid-mobilized elements.

the Sm–Nd results, yielding a 0.68 ± 0.19 Ga error-chron (M.S.W.D.=6.4, Model 3) but with excess scatter that we ascribe to heterogeneity in initial $^{176}Hf/^{177}Hf$. The strongly positive initial ε_{Hf} (+9.9 to +14.7) and ε_{Nd} (+5.6 to +7.9) of Groups I and II (Supplementary Table 2) indicate that their precursors were derived by melting ancient depleted mantle. Furthermore, these samples cluster tightly within the estimated MORB field (Fig. 4b) at 0.72 Ga, with the Group I eclogites being isotopically indistinguishable from the Group I gabbros, which, in conjunction with spatial relationships, and textural and chemical evidence, firmly establishes that the precursors of the gabbros and eclogites were cogenetic.

One Group II eclogite (Z309-5) has a Hf–Nd isotopic composition within the range of the Group I rocks, whereas two others (Z143-8, Z135-2) have distinctly lower $\varepsilon_{Nd}(t)$ than all other samples (i.e., +5.6 and +5.9). It is not clear whether these outliers are due to different source characteristics or the result of open-system behavior during the fluid-controlled LREE depletion. As reasoned below, the depletion probably occurred either during or before the gabbro-to-eclogite conversion.

Garnets from four Group II eclogites were analyzed to compare the internal isochron systematics of Lu–Hf and Sm–Nd systems. The garnet ages of the Lu–Hf (Fig. 5) and Sm–Nd [8] systems range from 595 to 672 Ma. Importantly, for the three samples where both types of ages were obtained, the ages agree (Z309-5: Sm–Nd, 595 ± 10 Ma, Lu–Hf, 607 ± 14 Ma; Z143-8: Sm–Nd,

638 ± 61 Ma, Lu–Hf, 619 ± 9 Ma; Z135-2 Sm–Nd 672 ± 14, MSWD 0.019, this study, Lu–Hf Grt-omph 659 ± 14 Ma). Because petrographic evidence implies that the first metamorphic reactions in these rocks occurred under eclogite facies conditions [3], we interpret these concordant ages to date garnet
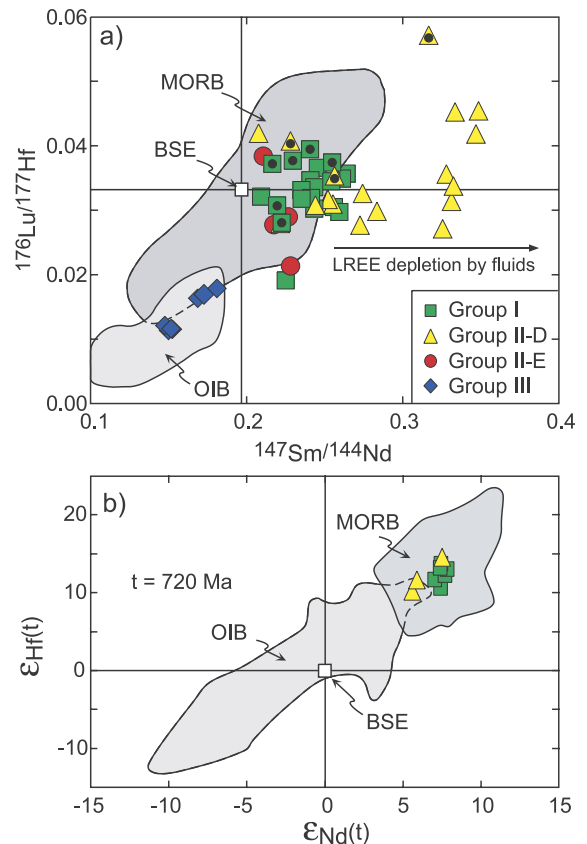

Fig. 4. (a) $^{176}Lu/^{177}Hf$ vs. $^{147}Sm/^{144}Nd$ of the Zambian eclogites and gabbros. Data are shown with generalized fields for modern basalts. Black dots mark samples for which Lu–Hf and Sm–Nd isotopic measurements were made; concentrations of these elements were measured by isotope dilution. MORB and OIB fields are based on the online databases http://georoc.mpch-mainz.gwdg.de, and http://petdb.ldeo.columbia.edu/petdb/ as well as data sources listed in Fig. 2 of [59]. (b) Hf–Nd isotope compositions of the Zambian eclogites and gabbros at 720 Ma relative to the terrestrial Hf–Nd mantle array. MORB and OIB fields are based on data from [60,61] and references therein. The positions of the fields were approximated by calculating Hf and Nd isotope compositions at 720 Ma assuming $^{176}Lu/^{177}Hf$ and $^{147}Sm/^{144}Nd$ ratios of ~0.039 and ~0.22, respectively, for their mantle sources. Bulk Silicate Earth (BSE) is assumed to be chondritic with respect to Lu–Hf and Sm–Nd.
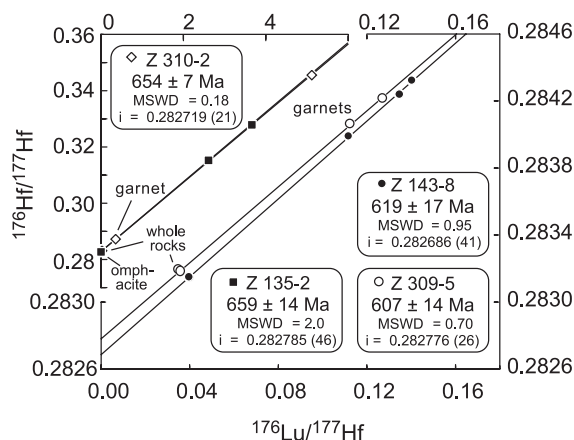
Fig. 5. Lu–Hf Grt–WR isochrons for Zambezi Belt eclogites. Samples Z310-2 and Z135-2 are plotted on a different scale than the other samples. Errors on $^{176}Lu/^{177}Hf$ and $^{176}Hf/^{177}Hf$ used in regressions are 0.2% and 2 S.E. internal run statistics ×2.3 (~2 S.D. external reproducibility) except for Z310-2 grt 2, and Z135 Grt 1 and 2 and Omp 1 and 2, where uncertainties for $^{176}Lu/^{177}Hf$ are ~1% because these samples were digested in Savillex® vials on a hotplate rather than in bombs. The Z135-2 regression includes the omphacites, but not the WR because it lies significantly off the isochron. We believe this is due to an inherited Hf component in the WR, presumably hosted by zircon or rutile, that did not equilibrate with Grt and Omph during metamorphism. The uncertainties of initial $^{176}Hf/^{177}Hf$ compositions (i) are 2 S.D. in the last digits. Regressions were calculated after [62].

growth during the fluid-triggered eclogitization. Given that Sm and Nd were more mobile than Lu and Hf in the Group II rocks, we consider the Lu–Hf chronometer to be more robust against disturbance by fluid infiltration in this case. The close agreement between Lu–Hf and Sm–Nd ages is therefore consistent with a scenario in which the fluid influx that caused up to seven-fold LREE depletions in the Group II samples occurred during eclogitization.

5. Discussion

5.1. Immobile trace element ratios: constraints on the mantle source and melting

The petrology and MORB-like REE and HFSE compositions of the Group I eclogites and gabbros suggest that they were part of a subducted oceanic plate (Figs. 2 and 3). Both Group I gabbros and

eclogites lie in the MORB field in incompatible element ratio diagrams (Figs. 4 and 6), and we therefore conclude that their precursor rocks formed at an oceanic spreading axis. Most samples lie on the trend of East Pacific Rise (EPR) MORB in a diagram of Hf/Yb vs. Nb/Zr (Fig. 6), implying that the observed variations within Group I are due to magmatic processes. The most depleted rocks were probably derived from a highly depleted mantle source or by high degrees of partial melting of depleted spinel peridotite. The negative Eu anomalies in Group I samples may be due to plagioclase fractionation. Similar anomalies are observed in the isotropic gabbro section of oceanic crust, whereas gabbros from the layered cumulate part display positive Eu anomalies due to plagioclase accumulation [31]. Consequently, the depleted MORB-type gabbroic rocks of Group I most likely represent former non-cumulate gabbros from lower oceanic crust that was subducted at ca. 0.6 Ga.

The LREE contents of the Group II eclogites are decoupled from those of the HREE and HFSE, which are present in concentrations similar to those of Group I samples (Fig. 2). Furthermore, both groups have similar positive initial Nd and Hf isotope compositions and similar Hf/Yb and Nb/Zr ratios (Figs. 4 and 6). We conclude that the magmatic precursors of
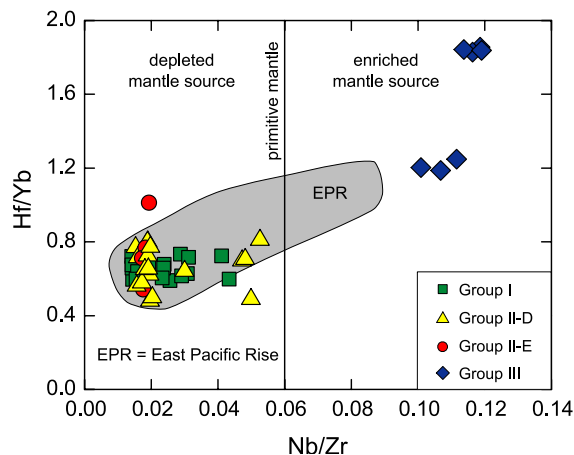

Fig. 6. Plot of Hf/Yb vs. Nb/Zr showing that the rocks of the Groups I and II resemble East Pacific Rise (EPR) MORB. In contrast, the Group III rocks are bimodal and they either follow an enriched plume influenced MORB trend that can be extrapolated from the EPR trend, or they follow an OIB trend, indicated by higher Hf/Yb ratios that are suggestive of residual garnet in the source.

Groups I and II were derived from similar depleted upper mantle sources but that the LREE compositions of the Group II samples have been disturbed. Magmatic processes alone do not decouple the LREE from the HREE and HFSE (Fig. 4). Instead, the observed fractionation in the Group II eclogites must have occurred during reaction of the rocks with an aqueous fluid. For example, both LREE-enriched and depleted eclogites occur at location Z143 and their complementary LREE patterns suggest that parts of this eclogite locality acted as sources—and others as sinks—for LREE (Fig. 3). The fluid-immobile elements Ta, P, Hf, and Ti behave similarly to the LREE during magmatic processes (i.e., partial melting and crystal fractionation) and were therefore used as bracketing elements to estimate the pre-depletion LREE concentrations (indicated with an asterisk, e.g., Ce*) of the Group II rocks in the same manner that Eu* is calculated from Sm and Gd. The similarity between the Group II LREE* concentrations and those of the depleted Group I LREE is consistent with a magmatic genesis of the two groups on a mid-oceanic ridge. High initial ε_{Nd} and ε_{Hf} values and the 595–659 Ma Sm–Nd and Lu–Hf ages suggest that Groups I and II were derived from a long-term depleted-mantle source and were subducted during a long-lived convergence in the Neoproterozoic. The petrologic evidence suggests that the rocks were subducted unmetamorphosed, with metastable mineral assemblages, to depths of >90 km, where fluid infiltration led to partial eclogitization of the middle oceanic crust [3]. The similarity of the initial Group II Nd isotope composition to that of the Group I rocks suggests that the fluid affecting the rocks must have had a comparable Nd isotopic composition to the basaltic and gabbroic protoliths.

In contrast to Groups I and II, the enriched rocks of Group III are more heterogeneous, with samples from localities Z140 and Z141 having significantly higher Hf/Yb for a given Nb/Zr compared to the Z145 samples (Fig. 6). Enriched precursor magmas may have been derived from an enriched source or by low degrees of partial melting in the mantle [32]. Though assimilation of continental crust could also generate enriched compositions, such assimilation by the Group III precursor magmas is unlikely because the samples lack strong LREE enrichment at constant HREE (i.e., $[Tb/Lu]_N \approx 1$) and negative Nb and Eu

anomalies (Fig. 2). Rather, the high OIB-like Nb contents (Fig. 7a) and the low HREE contents (<10×chondritic) of these rocks suggest their basaltic precursors formed by either low-degree partial melting of a spinel peridotite or melting of a garnet-bearing mantle source. For example, 5–15% partial melting of garnet peridotite could produce the observed range of $(La/Lu)_N$ for the Group III samples, with lower degrees of partial melting resulting in higher $(La/Lu)_N$ [33]. On the basis of their occurrence together with the MORB-like Group I and II samples and the lack of evidence for assimilated continental crust, we suggest that the Group III precursor rocks
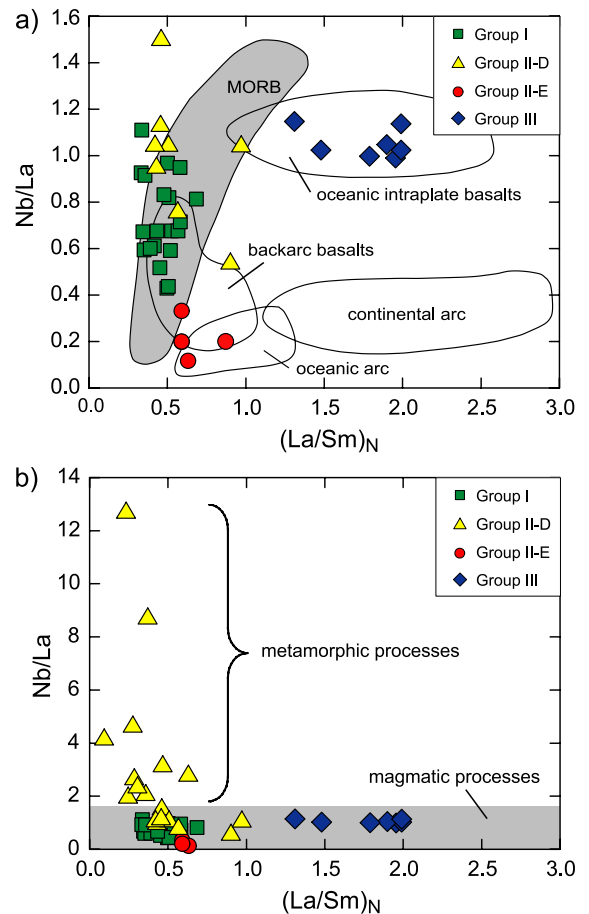

Fig. 7. (a) Plot of Nb/La vs. $(La/Sm)_N$ after John et al. [8] suggesting an origin of the mafic rocks of central Zambia at a mid-ocean ridge environment combined with the formation of rare ocean island basalts. (b) The high Nb/La ratios of some of the group II-D samples are out of the magmatic range and are the result of the fluid-induced eclogitization of these rocks.

were OIBs or enriched MORBs, and therefore parts of the oceanic lithosphere. Group III rocks only occur in a small part of the study area (Fig. 1) and most likely shared the same subduction and exhumation history, regardless of whether they were transformed to eclogites or not [3].

5.2. Mobile trace elements: constraints on fluid–rock interaction

During basalt genesis, parent/daughter ratios of the Lu–Hf and Sm–Nd systems are fractionated in the same sense, resulting in a strongly correlated array for basaltic lavas (Fig. 4a). Deviations from this array indicate post-magmatic element mobility. While such mobility was insignificant in the Group I rocks, most Group II-D samples show strongly increased Sm/Nd ratios due to LREE depletion by aqueous fluids. Likewise, samples from Groups I and III plot mostly within the fields of modern MORB and OIB in the Nb/La vs. $(La/Sm)_N$ diagram (Fig. 7a), whereas many Group II samples show La mobility relative to Nb and lie either below (Group II-E; Fig. 7a) or above (Group II-D; Fig. 7b) the magmatic trends. Uranium is highly fluid-mobile in oxidizing environments and the average U/Nb ratio of MORB and OIB is constant at about 0.02 [34]. Most Zambian gabbros fall close to this ratio, consistent with very little reaction of these rocks with an aqueous fluid (Fig. 8). On the other

hand, with the exception of one gabbro (Z138-10), all samples that plot outside the ocean basalt range (e.g., EPR) are eclogites, indicating a significant enrichment or, more rarely, depletion of U relative to Nb. In contrast, the unmetamorphosed gabbros retained their original U/Nb values. We conclude that the eclogite facies fluid–rock interaction fractionated the LREE as well as U and Th from the HFSE and HREE (Figs. 2 and 8). The gabbro-to-eclogite transformation is characterized by dissolution of the magmatic mineral assemblage by the infiltrating aqueous fluid and precipitation of the metamorphic mineral phases from this fluid. This implies that all elements were in solution and in equilibrium with the fluid, at least in subdomains [3] and hence, the additional uranium and thorium were probably incorporated into newly formed rutile and zircon.

Whereas most Group II samples were LREE-depleted by fluid infiltration during eclogitization, many are enriched in the more fluid-mobile elements, e.g., Rb and Ba, relative to MORB (Fig. 2), perhaps due to a second fluid infiltration during exhumation and retrograde metamorphism. Indeed, two fluid infiltration events can be resolved using Ce/Pb vs. 1/Pb relationships (Fig. 9). All samples except one have Ce/Pb lower than most MORB and OIB (i.e., 25 ± 5 [34]) implying alteration of the Ce/Pb by fluid(s). As previously outlined, fluid infiltration triggered the eclogitization of the two types of precursor basalts: depleted MORB and enriched MORB or OIB (end-members I′ and III′, respectively, in Fig. 9). This first fluid also redistributed the LREEs in some of the MORBs, producing LREE-depleted and LREE-enriched eclogites (endmembers II-D′ and II-E′, respectively, in Fig. 9). None of these endmember compositions is observed in the sample set. Instead, the samples define linear trends that fan out from the origin in Fig. 9 toward the endmembers of their respective groups, with the trends of Groups II-E and III being essentially identical because both are derived from enriched endmembers. The overall pattern is consistent with the passage of a second fluid that added Pb to rocks of all four groups, while leaving Ce concentrations relatively undisturbed (i.e., Ce/Ce* of Groups I and III do not vary as a function of Pb content). We infer that the second fluid was Pb-rich and probably derived from the dissolution of metasediments. Infiltration of the eclogites and gabbros by such a fluid most likely
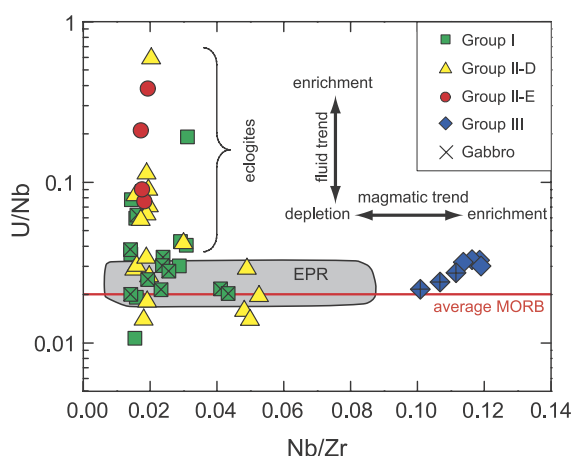

Fig. 8. Plot of U/Nb vs. Nb/Zr. All rocks having U/Nb ratios different than those of ocean basalts (e.g., EPR) [34] are eclogites. In contrast, all gabbros and only some eclogites have ratios similar to EPR.
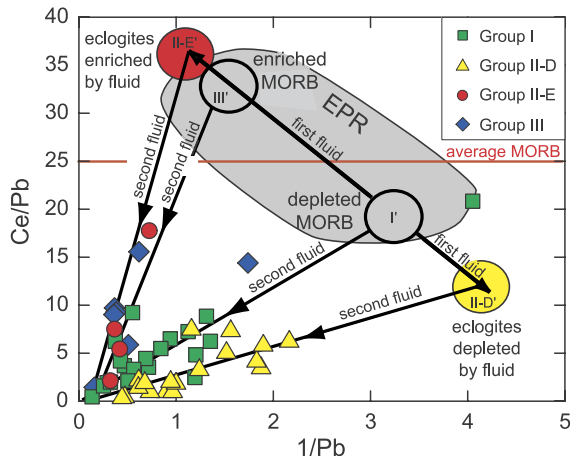
Fig. 9. Ce/Pb vs. 1/Pb showing two separate fluid-infiltration events. The first fluid is related to the eclogitization and the LREE-fractionation of Group II rocks, while the second fluid was Pb-rich and affected all samples, eclogites and gabbros, in that such that all samples lie on the Pb-rich ends of trends leading to the pre-second fluid endmembers of their corresponding groups (I′, II-D′, II-E′, III′). Average MORB value is from [34]. (Note: the exact positions of endmembers II-E′ and II-D′ along the trends are unconstrained because the effect of the first fluid on Pb has been masked by the second fluid infiltration. Positions shown are for illustration purposes only.)

occurred during exhumation in the subduction channel or during the later continental collision, and may be related to the amphibolitization or scapolitization that affected some samples. It is important to note that such retrograde reactions cannot be solely responsible for producing the LREE depletion and enrichment of the Group II rocks because (1) not all fluid-affected samples show late-stage amphibolitization, (2) gabbros that are amphibolitized do not show enrichment or depletion of the LREE by fluids, (3) all rocks in which the LREE were mobilized by fluids are eclogites, and (4) several eclogites are strongly depleted in LILE, implying no significant late stage fluid–rock interaction. Consequently, the remainder of the discussion focuses on the origin of the first fluid, which triggered eclogitization.

5.3. The composition of the fluid

The depletion of the LREE by fluids in the Group II rocks may have been possible because of the absence of epidote minerals, especially allanite, which usually act as sinks for these elements (e.g., [35,36]).

Prograde epidote minerals were only observed within a fluid infiltration vein found in one eclogite of Group II-E (Z310-4). It is noteworthy, however, that prograde epidote minerals, which should have been stable under the given P–T conditions, in a water-saturated, Al-rich basaltic system [37], are absent in all other eclogites. The lack of epidote minerals might be due to a reduced water-activity, low oxygen-fugacity of the infiltrating fluid, or the bulk composition of the subdomains in which the eclogitization took place [3]. Evidence for variable salinities of the infiltrating fluids was found in the form of variable Cl-contents of apatites, amphiboles, and phengites of different samples [3]. It is possible that a high Cl-activity only allows, in addition to the growth of Cl-rich apatite, the growth of rare Cl-bearing phengites and amphiboles, mineral groups that retain only minor amounts of LREE (e.g., [38]) and are found at only a few localities in the study area. A hydrous, Cl-bearing fluid for the whole Zambian suite is consistent with fluid inclusion studies that have found aqueous fluids of variable salinity and minor N_2 and CO_2 contents in a broad range of eclogite facies rocks [39,40].

5.4. Fluid–rock interaction modeling

John and Schenk [3] hypothesized that all of the rocks in the present study had been subducted, but gabbros only transformed to eclogites if they were infiltrated by fluid under eclogite facies conditions. Thus the eclogites and their veins represent relict fluid pathways through the subducted oceanic crust. The volume of fluid involved in eclogitization provides a key constraint for determining the fluid's source. We used the equations of Nabelek [41], together with fluid–rock partition coefficients (Supplementary Table 3) to estimate the amount of fluid that reacted with a gabbroic precursor to generate the observed chemical variations among the Group II eclogites. In this model, successive, infinitesimal fluid fractions infiltrate a metastable gabbro of MORB-like bulk composition under eclogite facies conditions and each fluid fraction fully reacts with the rock before leaving the system. We use partition coefficients for pure H_2O because (1) fluid inclusions in eclogites derived from oceanic crust have variable but usually low-salinities (in contrast to eclogitic high-salinity fluids of subduction zones in which also continental crust was

subducted) [42], (2) the effect of Cl on partition coefficients remains controversial [43–45] and (3) at eclogite facies conditions, aqueous fluids are strongly dissociated such that H_2O dominates their chemical properties [42,46].

Stalder et al. [44] showed experimentally that the internal trace element fractionation increases with decreasing temperature at high pressures, such that the contrast in partitioning behavior between highly incompatible elements (e.g., LREE) and the moderately incompatible elements (e.g., HREE) increases. In Fig. 10, Ce and Zr represent the LREE and HFSE, respectively. Although the HFSE are slightly mobile over short distances, e.g., during vein formation in eclogites [47], the lack of Zr fractionation relative to average MORB in these rocks suggests that the concentrations of Zr and most likely the other HFSE have not been affected by fluid (Supplementary Table 1, Figs. 2 and 4). Most of the HFSE content of eclogites may reside within rutile and zircon (e.g., [44]) and therefore the HFSE are not readily mobilized by fluids when these minerals are stable. For modeling fluid–rock ratios, we used Zr, an HFSE, as an immobile element against which the fluid-
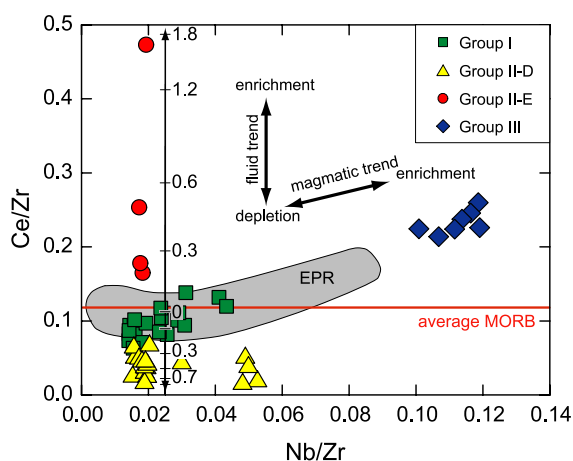

Fig. 10. Ce/Zr vs. Nb/Zr showing fluid–rock ratio modelling. Ce represents the fractionated LREE while Zr and Nb (both HFSE) are fluid-immobile reference elements. The model scale bar indicates the fluid–rock ratio needed to reproduce either the measured LREE enrichment or depletion from a gabbroic precursor. For a detailed description of the model, see text. Average MORB value is from [34]. The initial Ce/Zr ratios for the fluid–rock ratio modeling (i.e., fluid–rock ratio of 0) of depletion and enrichment differ (0.11 and 0.08, respectively) due to using different sample compositions. For clarity, only the initial Ce/Zr of the depletion calculation is shown.

mobile Ce is referenced. Calculated Ce* for the Group 2 eclogites are used as estimates of the initial Ce contents of their gabbroic precursors. Model Ce/Zr ratios resulting from depletion at different fluid–rock ratios are indicated on the scale bar drawn among Group II-D samples in Fig. 10. For the initial gabbro composition we used a Ce*/Zr ratio of 0.11 (from Z139-6; Ce* is the model pre-fluid infiltration Ce content calculated from the elements Ta_N and P_N as outlined above), which is consistent with the average N-MORB Ce/Zr (ca. 0.12 [48]). Because apatite occurs mostly in veins and might not be in equilibrium with the host rock, we considered only garnet, omphacite, and rutile when modeling fluid–rock ratios. Applying the D-values for 1000 °C and 5.0 GPa [44] (Supplementary Table 3) requires more than 80% fluid relative to the mass of the affected rock to produce the most depleted compositions (Fig. 10). However, the Zambian eclogites formed at 600–690 °C and 2.6–2.8 GPa, i.e., at much lower P and T than in the experiments of Stalder et al. [44]. For this reason, we also present fluid–rock ratios based on significantly higher D-values, which would be more realistic at those P–T conditions (R. Stalder, pers. comm.; Supplementary Table 3). In this case, less fluid is required, but still ca. 20% of the rock mass. We consider this amount to be a firm minimum because substituting the pure H_2O fluid with one that initially contained trace amounts of LREE (e.g., 2 ppm Ce) before interacting with the rock would increase the amount of fluid required to deplete the rocks to 110% and 21%, respectively. Furthermore, we assumed that Zr-contents remained constant throughout the continuous fluid–rock interaction; any leaching of Zr from the real rock samples by the fluid would lead to an underestimation of the fluid–rock ratio.

The LREE-enriched samples from localities Z143, Z140, and Z310 were modeled assuming that a fluid, which had previously scavenged LREE, infiltrated a pristine metastable gabbro (e.g., Z143-1, Ce*/Zr=0.08). Using this evolved fluid (Ce=26.5 ppm with literature D-values or 113 ppm with pers. comm. D-values, respectively) and the same mineral assemblage as in the depletion calculations, it is impossible to reproduce the observed Ce enrichments in the Group II-E rocks. To develop such high LREE enrichments, these rocks would have to contain at

least one additional mineral that could act as a LREE sink. Electron microprobe element mapping of Ce in our samples revealed that LREE-bearing minerals such as allanite, the most prominent carrier of REEs in eclogites [35,36] are absent in the Zambian rocks and that prograde epidote minerals are found in only one Group II-E sample (Z310-4). However, apatite, which is part of the vein- or matrix assemblages [3], may dominate the LREE reservoirs in eclogites if epidote minerals are absent [35,38]. If 1.5% apatite is included in the model assemblage, the amount of fluid that must have reacted with a pristine gabbro to form the Group II fluid-enriched rocks would have been ca. 170% and >21%, using partition coefficients from Stalder et al. [44] and Stalder, pers. comm., respectively. Although the LREE enrichment process seems to be straightforward for epidote-bearing Z310-4 sample, it is more difficult to explain for other samples, especially those from locality Z143, where no clear petrologic indicators were found that could explain why some samples are enriched while the others are depleted.

The modeling is consistent with the decoupling of LREE from the HREE and HFSE being due to a large fluid flux through the system. Using all trace elements for modeling, the resulting trace element patterns of the fluid are similar to those of Stalder et al. [44] (their Fig. 9), with the exception of the HREE, which were mobilized in their model because they used rutile and clinopyroxene, but not garnet. The HREE and HFSE are relatively immobile if garnet, rutile, and zircon are prograde minerals, which is indicated for the Zambian rocks by tiny (<5 μm) rutile and zircon inclusions in garnet. However, for the Zambian eclogites omphacite is the main carrier of LREE and its affinity for the LREE may not be high enough to prevent leaching by aqueous fluids. In contrast to the mechanisms responsible for LREE-leaching, those behind the LREE-scavaging process are poorly understood and difficult to explain with the observed mineral assemblages (Z310-4 is an exception). However, the large volumes of fluid that infiltrated the metastable mineral assemblages of the mafic rocks reacted only for short time periods and, in some cases only within small, scattered subdomains of the affected rocks, with large portions of the rocks never reaching equilibrium conditions. In some of these subdomains, Ky-bearing garnet–omphacite assemblages formed even though these MORB-type rocks have Al-poor compositions [3]. Thus, element transport during open-system metamorphism may not be only governed by simple equilibrium fluid–mineral partitioning. Instead, the element transport in the subducting lithosphere appears to be largely controlled by fluid–rock ratios. However, fluid flow velocities, and the coupled processes of precursor assemblage dissolution and HP assemblage precipitation, which are sensitive to pressure, temperature, and fluid chemistry, may also play a role but have not been quantified yet.

5.5. The source of the fluid

Fluids in subduction zones may originate from sediments, altered basaltic crust, or serpentinized mantle. For the Zambian rocks, the first fluid infiltrated the rocks under eclogite facies conditions at depths >90 km [3]. By the time the slab reaches these conditions, the oceanic crust and the sediments have lost almost all of the water that can be released during burial to subarc-depths (ca. 90–140 km) [37,49]. The depletion of mobile elements in some of the eclogites implies that the fluid must have been strongly undersaturated in LREE and LILE. In contrast, sediment-derived fluids would have high LILIE and LREE concentrations and would have significantly lowered the initial Nd isotope compositions of the Zambian rocks. Likewise, fluids derived from altered basaltic crust should also be very enriched in LREE and LILE. Sediments and altered basaltic crust are therefore unlikely fluid source candidates [43]. Our estimated fluid–rock ratios require an amount of fluid that is apparently too high to have originated in the slab's lower crust because the gabbroic part of the oceanic crust is usually not intensively altered (≤30%) and contains <1.5 wt.% H_2O [37,50]. We conclude that the fluid that triggered the eclogitization and fractionated the LREE cannot be derived from the sediments or subducted crust, leaving the serpentinized mantle portion of the slab as the most likely fluid source. Schmidt and Poli [37] calculated that serpentinization of 10% of the upper 5 km of the mantle beneath the oceanic crust leads to approximately twice the amount of water in this part of the slab than exists in the entire overlying section of oceanic crust. This serpentinized mantle would start to dehydrate at depths greater than 100 km (e.g. [49]),

necessitating the rapid transport of fluids over several kilometers within the slab to the site of eclogitization, which in turn implies that the fluid flow is channelized, most likely along fractures.

5.6. Fluid pathways and fluid transport into the mantle wedge

Our proposed fluid source requires several-kilometer long distances of fluid transport, i.e., from serpentinized lithospheric mantle upwards through the entire subducting crust, rather than the meter-scale or even shorter distance transport suggested for other HP subduction zone rocks [40,51]. These authors proposed that the channels of fluid escape from the slab to the mantle wedge may not have been identified yet. This could be because the HP veins described so far represent locally buffered dehydration and transport veins (e.g., [52]) that are merely tributaries to the main pathways. These pathways may have formed along reactivated fracture zones [53], where faulting is facilitated by high fluid pore pressures, which decrease friction [54]. Evidence for the existence of slab fluid flow caused by such hydrofracturing has been found in the blueschist of the Tianshan [52].

The dehydration of a slab is a continuous process that starts at 10–20 km and persists to depths greater than 300 km (e.g., [37]). According to the model of Gerya et al. [55], slab fluids released at depths up to 100 km hydrate part of the overlying wedge, forming a subduction channel consisting of serpentinized mantle. These shallow slab fluids may become trapped in the subduction channel, unable to reach the region were arc magmas are generated in the mantle wedge. In contrast, fluids released from the dehydration of serpentinized slab-mantle enter the wedge at depths greater than 100 km (e.g., [49]) and therefore probably are not trapped within the subduction channel. However, these fluids must traverse the entire oceanic crustal section before entering the mantle wedge, and they are the most likely catalysts for the gabbro-to-eclogite transformation and LREE fractionation observed in the Zambezi Belt eclogites. Fig. 11 shows that typical island arc basaltic magmas are enriched in the LREE as well as in the LILE relative to the immobile HFSE. Thus, these magmas have trace element signatures that are complementary to the Zambian eclogites, suggesting that fluids that have reacted with eclogite can be responsible
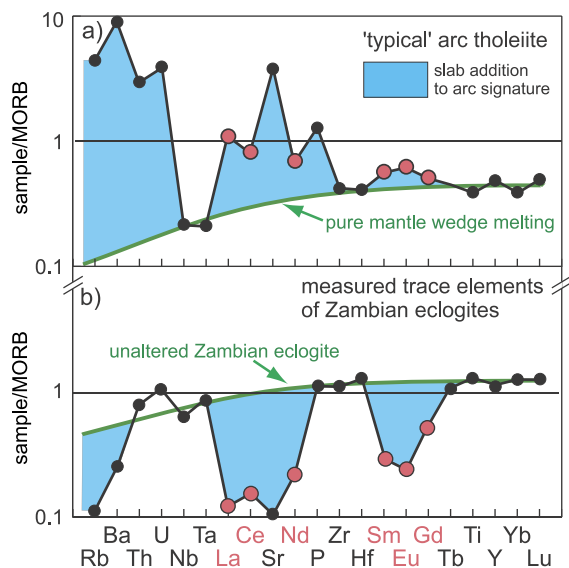

Fig. 11. MORB-normalized patterns of 'typical' arc tholeiite [63] (a) and Zambian eclogite (Z139-6) (b) show that several of the elements in the slab component of arc magmas have been removed from the Zambian eclogites by fluids. The LREE are highlighted.

for generating the slab component in arc magmas (Fig. 11). We conclude that the transformation of dry, metastable slab gabbros to eclogites upon fluid-infiltration results in large-scale fluid transport of mobile elements to the sub-arc mantle.

6. Conclusions

(1) The magmatic precursors of the Zambezi Belt gabbros and eclogites are cogenetic, with compositional variations from very depleted- to enriched MORB as well as OIB. They represent pieces of the gabbroic part of subducted oceanic crust.
(2) The range of Lu–Hf garnet-whole rock ages represented by the four dated eclogites suggest that subduction was long-lived, at least 24 Ma.
(3) Identical Lu–Hf and Sm–Nd ages and the fact that only eclogites were enriched or depleted in LREE suggest that eclogitization and LREE fractionation occurred contemporaneously.
(4) Eclogitization and LREE fractionation are due to channelized fluid infiltration. The observed degrees of LREE fractionation require high fluid–rock ratios of up to 80%.

(5) The mobility of the LREE in subduction zone environments depends on the stability and presence of mineral phases that incorporate the LREE. The lack of epidote group minerals may be caused either by low a_{H_2O} or low f_{O_2} of the acting fluid during the initial phase of eclogitization.

(6) The most likely source of the eclogitization-triggering fluid is the serpentinized mantle beneath subducting oceanic crust. This requires a long distance transport (several km) through the slab.

(7) The dehydration of the slab serpentinites, coupled with the selective trace element mobilization that occurs during gabbro-to-eclogite transformation, may be more important for generating the slab component of arc magmas than the dehydration of blueschists.

(8) A second, Pb-rich fluid reacted with the gabbros and eclogites, probably within the subduction channel during their ascent or during the following continental collision.

Acknowledgements

Appendix A. Supplementary data

Supplementary data associated with this article can be found, in the online version, at doi:10.1016/j.epsl.2004.09.009.

References

[1] B.R. Hacker, Eclogite formation and the rheology, buoyancy, seismicity, and H$_2$O content of oceanic crust, in: G.E. Bebout, D.W. Scholl, S.H. Kirby, J.P. Platt (Eds.), Subduction Top to Bottom, Geophysical Monograph, vol. 96, American Geophysical Union, Washington, 1996, pp. 337–346.

[2] H. Austrheim, Influence of fluid and deformation on metamorphism of the deep crust and consequences for the geodynamics of collision zones, in: B.R. Hacker, J.G. Liou (Eds.), When Continents Collide: Geodynamics and Geochemistry of Ultrahigh-Pressure Rocks, Kluwer Academic Publishers, 1998, pp. 297–323.

[3] T. John, V. Schenk, Partial eclogitisation of gabbroic rocks in a late Precambrian subduction zone (Zambia): prograde metamorphism triggered by fluid infiltration, Contributions to Mineralogy and Petrology 146 (2003) 174–191.

[4] J.B. Gill, Orogenic Andesites and Plate Tectonics, Springer Verlag, Berlin, 1981.

[5] Y. Tatsumi and S.M. Eggins, Subduction zone magmatism (1995) 211.

[6] C.J. Hawkesworth, K. Gallagher, J.M. Hergt, F. McDermott, Mantle and slab contributions in arc magmas, Annual Review of Earth and Planetary Sciences 21 (1993) 175–204.

[7] M.R. Perfit, D.A. Gust, A.E. Bence, R.J. Arculus, S.R. Taylor, Chemical characteristics of island-arc basalts; implications for mantle sources, Chemical Geology 30 (1980) 227–256.

[8] T. John, V. Schenk, K. Haase, E. Scherer, F. Tembo, Evidence for a Neoproterozoic ocean in south-central Africa from mid-oceanic-ridge-type geochemical signatures and pressure–temperature estimates of Zambian eclogites, Geology 31 (2003) 243–246.

[9] J. Bernard-Griffiths, J. Cornichet, Origin of eclogites from South Brittany, France; a Sm–Nd isotopic REE study, Chemical Geology 52 (1985) 185–201.

[10] A. Möller, P. Appel, K. Mezger, V. Schenk, Evidence for a 2 Ga subduction zone; eclogites in the Usagaran Belt of Tanzania, Geology 23 (1995) 1067–1070.

[11] J. Bernard-Griffiths, J.J. Peucat, R.P. Menot, Isotopic (Rb–Sr, U–Pb and Sm–Nd) and trace element geochemistry of eclogites from the Pan-African Belt; a case study of REE fractionation during high-grade metamorphism, Lithos 27 (1991) 43–57.

[12] H. Becker, K.P. Jochum, R.W. Carlson, Trace element fractionation during dehydration of eclogites from high-pressure terranes and the implications for element fluxes in subduction zones, Chemical Geology 163 (2000) 65–99.

[13] A. Brunsmann, G. Franz, J. Erzinger, REE mobilization during small-scale high-pressure fluid–rock interaction and zoisite/fluid partitioning of La to Eu, Geochimica et Cosmochimica Acta 65 (2001) 559–570.

[14] A.K. Engvik, H. Austrheim, M. Erambert, Interaction between fluid flow, fracturing and mineral growth during eclogitization, an example from the Sunnfjord area, Western Gneiss region, Norway, Lithos 57 (2001) 111–141.

[15] T. John, V. Schenk, K. Mezger, F. Tembo, Timing and *P–T* evolution of whiteschist metamorphism in the Lufilian Arc–Zambezi Belt orogen (Zambia): implication to the Gondwana assembly, Journal of Geology 112 (2004) 71–90.

[16] H. Porada, V. Berhorst, Towards a new understanding of the Neoproterozoic–early Palaeozoic Lufilian and northern Zambezi belts in Zambia and the Democratic Republic of Congo, Journal of African Earth Sciences 30 (2000) 727–771.

[17] M.L. Vinyu, R.E. Hanson, M.W. Martin, S.A. Bowring, H.A. Jelsma, M.A. Krol, P.H.G.M. Dirks, U–Pb and ${}^{40}Ar/{}^{39}Ar$ geochronological constraints on the tectonic evolution of the easternmost part of the Zambezi orogenic belt, Northeast Zimbabwe, Precambrian Research 98 (1999) 67–82.

[18] B. Goscombe, R.A. Armstrong, J.M. Barton, Geology of the Chewore Inliers, Zimbabwe; constraining the Mesoproterozoic to Palaeozoic evolution of the Zambezi Belt, Journal of African Earth Sciences 30 (2000) 589–627.

[19] S. Vrana, R. Prasad, E. Fediukova, Metamorphic kyanite eclogites in the Lufilian Arc of Zambia, Contributions to Mineralogy and Petrology 51 (1975) 139–160.

[20] C.D. Garbe-Schönberg, Simultaneous determination of thirty-seven trace elements in twenty-eight international rock standards by ICP-MS, Geostandards Newsletter 17 (1993) 81–97.

[21] C. Münker, S. Weyer, E. Scherer, K. Mezger, Separation of high field strength elements (Nb, Ta, Zr, Hf) and Lu from samples for MC-ICPMS measurements, Geochemistry Geophysics Geosystems 2 (2001) (2001GC000183).

[22] G. Gruau, J. Cornichet, M. Le Coz-Bouhnik, Improved determination of Lu/Hf ratio by chemical separation of Lu from Yb, Chemical Geology 72 (1988) 353–356.

[23] K. Mezger, E.J. Essene, A.N. Halliday, Closure temperatures of the Sm–Nd system in metamorphic garnets, Earth and Planetary Science Letters 113 (1992) 397–409.

[24] E. Scherer, C. Münker, K. Mezger, Calibration of the lutetium–hafnium clock, Science 293 (2001) 683–687.

[25] G.W. Lugmair, K. Marti, Lunar initial ${}^{143}Nd/{}^{144}Nd$; differential evolution of the lunar crust and mantle, Earth and Planetary Science Letters 39 (1978) 349–357.

[26] J. Blichert-Toft, F. Albarede, The Lu–Hf isotope geochemistry of chondrites and the evolution of the mantle–crust system, Earth and Planetary Science Letters 148 (1997) 243–258.

[27] S.B. Jacobsen, G.J. Wasserburg, Sm–Nd isotopic evolution of chondrites, Earth and Planetary Science Letters 50 (1980) 139–155.

[28] B.J. Wasserburg, S.B. Jacobsen, D.J. DePaolo, M.T. McCulloch, T. Wen, Precise determination of Sm/Nd ratios, Sm and Nd isotopic abundances in standard solutions, Geochimica et Cosmochimica Acta 45 (1981) 2311–2323.

[29] J.I. Wendt, M. Regelous, Y. Niu, R. Hekinian, K.D. Collerson, Geochemistry of lavas from the Garrett transform fault; insights into mantle heterogeneity beneath the eastern Pacific, Earth and Planetary Science Letters 173 (1999) 271–284.

[30] J. Blichert-Toft, F. Albarede, M. Rosing, R. Frei, D. Bridgwater, The Nd and Hf isotope evolution of the mantle through the Archean; results from the Isua supracrustals, West Greenland, and from the Birimian terranes of West Africa, Geochimica et Cosmochimica Acta 63 (1999) 3901–3914.

[31] S.R. Hart, J. Blusztajn, H.J.B. Dick, P.S. Meyer, K. Muehlenbachs, The fingerprint of seawater circulation in a 500-meter section of ocean crust gabbros, Geochimica et Cosmochimica Acta 63 (1999) 4059–4080.

[32] F.A. Frey, D.H. Green, S.D. Roy, Integrated models of basalt petrogenesis: a study of quartz tholeiites to olivine melilitites from south eastern Australia utilizing geochemical and experimental petrological data, Journal of Petrology 19 (1978) 463–513.

[33] G.N. Hanson, An approach to trace element modeling using a simple igneous system as an example, in: B.R. Lipin, G.A. McKay (Eds.), Geochemistry and Mineralogy of Rare Earth Elements, Reviews in Mineralogy, 1989, pp. 79–97.

[34] A.W. Hofmann, K.P. Jochum, M. Seufert, W.M. White, Nb and Pb in oceanic basalts: new constraints on mantle evolution, Earth and Planetary Science Letters 79 (1986) 33–45.

[35] R. Tribuzio, B. Messiga, R. Vannucci, P. Bottazzi, Rare earth element redistribution during high-pressure–low-temperature metamorphism in ophiolitic Fe-gabbros (Liguria, northwestern Italy); implications for light REE mobility in subduction zones, Geology 24 (1996) 711–714.

[36] J. Hermann, Allanite; thorium and light rare earth element carrier in subducted crust, Chemical Geology 192 (2002) 289–306.

[37] M.W. Schmidt, S. Poli, Experimentally based water budgets for dehydrating slabs and consequences for arc magma generation, Earth and Planetary Science Letters 163 (1998) 361–379.

[38] T. Zack, S.F. Foley, T. Rivers, Equilibrium and disequilibrium trace element partitioning in hydrous eclogites (Trescolmen, Central Alps), Journal of Petrology 43 (2002) 1947–1974.

[39] R. Klemd, M. Bröcker, Fluid influence on mineral reactions in ultrahigh-pressure granulites; a case study in the Snieznik Mts. (West Sudetes, Poland), Contributions to Mineralogy and Petrology 136 (1999) 358–373.

[40] M. Scambelluri, P. Philippot, Deep fluids in subduction zones, Lithos 55 (2001) 213–227.

[41] P.I. Nabelek, General equations for modeling fluid/rock interaction using trace element and isotopes, Geochimica et Cosmochimica Acta 51 (1987) 1765–1769.

[42] C.E. Manning, The chemistry of subduction-zone fluids, Earth and Planetary Science Letters 223 (2004) 1–16.

[43] J.M. Brenan, H.F. Shaw, F.J. Ryerson, D.L. Phinney, Mineral–aqueous fluid partitioning of trace elements at 900 degrees C and 2.0 GPa; constraints on the trace element chemistry of mantle and deep crustal fluids, Geochimica et Cosmochimica Acta 59 (1995) 3331–3350.

[44] R. Stalder, S.F. Foley, G.P. Brey, I. Horn, Mineral–aqueous fluid partitioning of trace elements at 900–1200 degrees C and 3.0–5.7 GPa; new experimental data for garnet, clinopyroxene, and rutile, and implications for mantle metasomatism, Geochimica et Cosmochimica Acta 62 (1998) 1781–1801.

[45] H. Keppler, Constraints from partitioning experiments on the composition of subduction-zone fluids, Nature 380 (1996) 237–240.

[46] S.D. Hamann, Properties of electrolyte solutions at high pressures and temperatures, in: D.T. Rickard, F.E. Wickman (Eds.), Physics and Chemistry of the Earth, vol. 13–14, Pergamon, 1981, pp. 89–111.

[47] D. Rubatto, J. Hermann, Zircon formation during fluid circulation in eclogites (Monviso, Western Alps): implications for Zr and Hf budget in subduction zones, Geochimica et Cosmochimica Acta 67 (2003) 2173–2187.

[48] A.W. Hofmann, Chemical differentiation of the Earth; the relationship between mantle, continental crust, and oceanic crust, Earth and Planetary Science Letters 90 (1988) 297–314.

[49] L.H. Rüpke, J. Phipps Morgan, M. Hort, J.A.D. Connolly, Are the regional variations in Central American arc lavas due to differing basaltic versus peridotitic slab sources of fluids? Geology 30 (2002) 1035–1038.

[50] K. Wallmann, The geological water cycle and the evolution of marine $\Delta^{18}O$ values, Geochimica et Cosmochimica Acta 65 (2001) 2469–2485.

[51] I. Cartwright, A.C. Barnicoat, Stable isotope geochemistry of Alpine ophiolites; a window to ocean-floor hydrothermal alteration and constraints on fluid–rock interaction during high-pressure metamorphism, International Journal of Earth Sciences (Geologische Rundschau) 88 (1999) 219–235.

[52] J. Gao, R. Klemd, Primary fluids entrapped at blueschist to eclogite transition; evidence from the Tianshan meta-subduction complex in northwestern China, Contributions to Mineralogy and Petrology 142 (2001) 1–14.

[53] S.H. Kirby, E.R. Engdahl, R.P. Denlinger, Intermediate-depth intraslab earthquakes and arc volcanism as physical expressions of crustal and uppermost mantle metamorphism in subducting slabs, in: G.E. Bebout, D.W. Scholl, S.H. Kirby, J.P. Platt (Eds.), Subduction Top to Bottom, Geophysical Monograph, vol. 96, American Geophysical Union, Washington, 1996, pp. 195–214.

[54] J.H. Davies, The role of hydraulic fractures and intermediate-depth earthquakes in generating subduction-zone magmatism, Nature 398 (1999) 142–145.

[55] T.V. Gerya, B. Stöckhert, A.L. Perchuk, Exhumation of high-pressure metamorphic rocks in a subduction channel: a numerical simulation, Tectonics 21 (2002).

[56] J.G. Thieme, Geological Map of the Lusaka Area, Map No. SD-35-15, Geological Survey of Zambia, Lusaka, 1984.

[57] W.V. Boynton, Cosmochemistry of the rare earth elements; meteorite studies, in: P. Henderson (Ed.), Rare Earth Element Geochemistry, Elsevier, Amsterdam, 1984, pp. 63–107.

[58] J.A. Pearce, Role of the subcontinental lithosphere in magma genesis at activ continental margins, in: C.J. Hawkesworth, M.J. Norry (Eds.), Continental Basalts and Mantle Xenoliths, Shiva Press, Nantwich, 1983, pp. 230–272.

[59] J. Blichert-Toft, F. Albarede, J. Kornprobst, Lu–Hf isotope systematics of garnet pyroxenites from Beni Bousera, Morocco; implications for basalt origin, Science 283 (1999) 1303–1306.

[60] V.J.M. Salters, W.M. White, Hf isotope constraints on mantle evolution, Chemical Geology 145 (1998) 447–460.

[61] C. Chauvel, J. Blichert-Toft, A hafnium isotope and trace element perspective on melting of the depleted mantle, Earth and Planetary Science Letters 190 (2001) 137–151.

[62] K.R. Ludwig, Isoplot/Ex version 2.49, A Geochronological Toolkit for Microsoft Excel, Berkeley Geochronology Center Special Publication 1a Nov. 20, 2001.

[63] D.W. Peate, J.A. Pearce, C.J. Hawkesworth, H. Colley, C.M.H. Edwards, K. Hirose, Geochemical variations in Vanuatu Arc lavas: the role of subducted material and a variable mantle wedge composition, Journal of Petrology 38 (1997) 1331–1358.